Biophysical Chemistry 254 (2019) 106249

Contents lists available at ScienceDirect

Biophysical Chemistry

journal homepage: www.elsevier.com/locate/biophyschem

Meso-Raman approach for rapid yeast cells identification

Martina Alunni Cardinali[a], Debora Casagrande Pierantoni[b], Silvia Caponi[c,*], Laura Corte[b], Daniele Fioretto[a,d], Gianluigi Cardinali[b,d]

[a] Department of Physics and Geology, University of Perugia, via Pascoli, I-06123 Perugia, Italy
[b] Department of Pharmaceutical Sciences, University of Perugia, via del Liceo 1, I-06123 Perugia, Italy
[c] Institute of Materials, National Research Council (IOM-CNR), Unit of Perugia, c/o Department of Physics and Geology, University of Perugia, Via A. Pascoli, I-06123 Perugia, Italy
[d] CEMIN-Excellence Research Center, University of Perugia, via Pascoli, I-06123 Perugia, Italy

HIGHLIGHTS

- A meso-Raman approach for yeasts cell identification
- Polarized and Depolarized Raman Spectra for PCA analysis
- Future efficient and reliable protocol for medical diagnosis in clinics

GRAPHICAL ABSTRACT

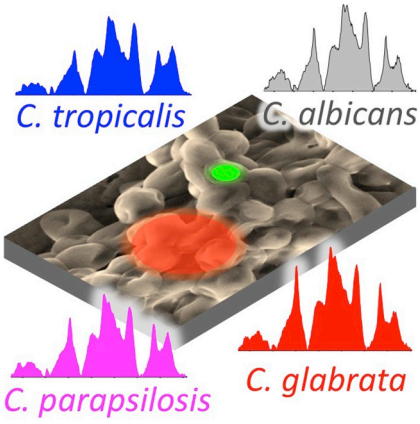

ARTICLE INFO

Keywords:
Raman microscopy
Vibrational spectroscopy
Light scattering
Candida yeasts
Phenotypic identification

ABSTRACT

An increasing effort is currently devoted to developing Raman spectroscopy for identification of microorganisms. Micro-Raman setups are typically used for this purpose with the limit that the intra-species and inter-species spectral variability are comparable, thus limiting the identification capability. To overcome this limit a meso-Raman approach is here implemented. Thin films of planktonic cells are analyzed throughout the collection of back-scattered light providing a Raman signal already averaged over tens of cells. The collecting of unpolarized (VU) and depolarized (HV) Raman signals increased the spectral information obtainable from the data, demonstrating the ability of the principal component analysis to differentiate the most common *Candida* species, namely *C. glabrata*, *C. albicans*, *C. parapsilosis* and *C. tropicalis*. The proposed method can contribute to bring Raman spectroscopy closer to its potential clinical use for fast identification of yeast cells.

* Corresponding author.
E-mail address: silvia.caponi@cnr.it (S. Caponi).

https://doi.org/10.1016/j.bpc.2019.106249
Received 6 June 2019; Received in revised form 13 August 2019; Accepted 13 August 2019
Available online 14 August 2019

1. Introduction

The spectroscopic characterization of whole microbial cells was introduced in the early 90s of the last century by Neuman and co-operators introducing the FTIR technology [1]. The concept was that a comprehensive chemometric description of the metabolome would allow the identification and the fingerprint of the strains. The technique was extended to MicroFTIR using small amounts of cells with the advantage of reducing the growth time necessary to prepare the biomass, heading to a single cell technique as a final target [2–6]. The presence of water is a difficult problem to solve with IR spectroscopy, which can be efficiently overcome by using Raman scattering. The introduction of this technique in microbiology paved the way to analyses of whole cells in their own (liquid) environment, with even the possibility to monitor them during their growth [7]. Whatever the technique, the application of spectroscopy to microbial taxonomy requires a careful microbiological modelling including: *i*) type strains of the species under investigation, *ii*), the awareness of the actual spatial resolution of the whole experimental approach. A type strain is the official representative of a species, normally deposited in important culture collections with the aim of being used as a reference in all taxonomic related works. Strains can be considered well identified and used to set-up an identification routine when the assignment to their actual species has been carried out with state of the art technology, which nowadays is represented by ITS marker in fungi [8]. Finally, the taxonomic resolution is the ability of a technique to separate strains of different species, while clustering those of the same species. In a recent paper [9], we were able to demonstrate that identification by means of FTIR requires sophisticated clustering procedures with statistical treatments to assess, whether strains of two related species are closer to the actual type strains of the species it belongs to or the type strain of the neighbor species. This showed that the use of spectroscopy as a convenient proxy of current molecular marker-based taxonomy requires a careful set up and the presence of type strains in the set of strains used.

Beyond the aspects outlined above, one has to take also into consideration that microbial eukaryotic cells undergo a four phases life cycle, during which the metabolome is likely to change both quantitatively and qualitatively. For instance, cells in G2 phase have twice as much DNA than in G1 or early S phase. This consideration means that single cells analysis could introduce a large variability due to the specific cell phase with obvious problems in terms of reproducibility and precision. For this reason, spectroscopy should be able to catch the signal from a rather large number of cells rather than from single ones.

In this context, Raman spectroscopy is progressively gaining consensus [10], since it offers the advantage of a relative insensitiveness to water, allowing for analyses in both dry and wet substrates, which can explore the whole range of possible physiological conditions. Raman spectra of microbial cells provide us with a chemical fingerprint of their phenotype and metabolic state, revealing the sum of signals from all the molecular species in the scattering volume [11,12]. An often overlooked aspect in whole-cell Raman spectroscopy is the actual biological resolution of the method, which stems from both microbiological factors, and technical settings, such as data acquisition and elaboration procedures [13,14]. It is therefore necessary to provide an accurate protocol for the whole process, starting from the culturing phase up to the chemometric analysis of the spectroscopic data, in order to obtain reproducible and significant data [15–18]. Different studies have already suggested that Raman micro-spectroscopic techniques are suitable for the identification of bacteria and yeasts [19–22], both by analyzing microcolonies (10–100 μm) and macrocolonies (> 100 μm) grown on a solid medium [20,22–26], and by analyzing single isolated cells [27–29]. These approaches, on one hand guarantee the rapid availability of the sample but, on the other hand, require a high degree of confocality. This is necessary to select the contribution of different portions of single cells and exclude the one of the culture medium. As a consequence, averaging over a large number of spectra is required, to account for the extremely heterogeneous landscape made by internal cellular portions, metabolic states, and colony's architectures [2,29].

In the present work, we carried out a proof-of-concept study based on a significant and well-defined biological model represented by the type strains of the four most important species among the pathogenic yeasts of the genus *Candida*, i.e. *C. albicans*, *C. tropicalis*, *C. parapsilosis* and *C. glabrata*. Whereas the first three are pre whole-genome-duplication (WGD) species [30], the last is a relative of *Saccharomyces cerevisiae* and derives from the genome duplicated ancestor. This knowledge gives the biological model a fully certified taxonomic status, as well as the possibility to quantitatively estimate the actual differences between strains. Moreover, *Candida* is currently deserving great attention and asking for fast identification since it is responsible for many of the nosocomial infections [31–34], which can become severe systemic infections, when the immune system is strongly compromised [35–37].

The analysis of eukaryotic cells provides an extremely demanding workbench, since they have nuclei well separated from other portions of the cell and a complex pattern of metabolic states, so that high variability among spectra derived from different portions of the same cell and from different cells of the same culture can be expected. For this reason, our aim is to define the critical aspects in yeast cell preparation, spectra measurements and data processing, in order to mitigate the sources of variation and propose a reliable procedure for rapid Raman identification of yeast cells.

2. Materials and methods

2.1. Sample preparation

Candida albicans CMC 1968, *Candida tropicalis* CMC 2052, *Candida parapsilosis* CMC 1841 and *Candida glabrata* CMC 2032, were isolated from nosocomial environments and used to optimize the measuring procedure. The identification of the strains was carried out by comparing the ITS and LSU D1/D2 sequences with GenBank (http://blast.ncbi.nlm.nih.gov/Blast.cgi) and specific databases. All strains are able to form biofilm in laboratory conditions [11]. In order to obtain the biomass, bottles containing 20 ml of YPD (Yeast Extract 1%, Peptone 1%, Dextrose 2%, − Difco Laboratories, Detroit, MI, USA) were inoculated with a loopful of cells from the stock cultures and incubated for 24 h at 37 °C. This procedure inhibits the formation of biofilm, thus increasing the homogeneity of the sample. Different aliquots were centrifuged and washed twice with saline solution (0.9% NaCl) and with pure HPLC water. The solutions were finally adjusted to an optical density OD = 30 with pure HPLC water.

To improve the accuracy in the identification process, the effects of different drying protocols on the quality and the shape of Raman spectra has been tested. In particular, we have analyzed thin pellets (few layers of cells supported on polished metallic substrates) left to dry at room temperature and heated at 42 °C for 15 min with and without a fixation phase in formalin with final concentration of 4% *W/V*. The fixation process has given negligible modifications to the shape of Raman spectra; we have therefore chosen to analyze fixed samples both to reduce the biological hazard and to reduce the metabolic heterogeneity of the samples.

Laser irradiation is associated with a fluorescence background, which can mask the Raman peaks related to molecular structures. Previous studies, on both *Candida* and other microorganisms, have already underlined that the quantity of water [29] and the physical fixation by heating can influence spectral features [38]; the molecular origin of this phenomenon is still not clear. In our samples, we observed that overwhelming fluorescence is associated with the presence of surface fractures developing in very thin (few micrometers thick) films obtained from low optical density solutions. In that case, small portions of thin sample films detached from the substrate might experience a lower thermal conduction, giving rise to a higher thermal degradation induced by laser irradiation. Analogously, very high fluorescence

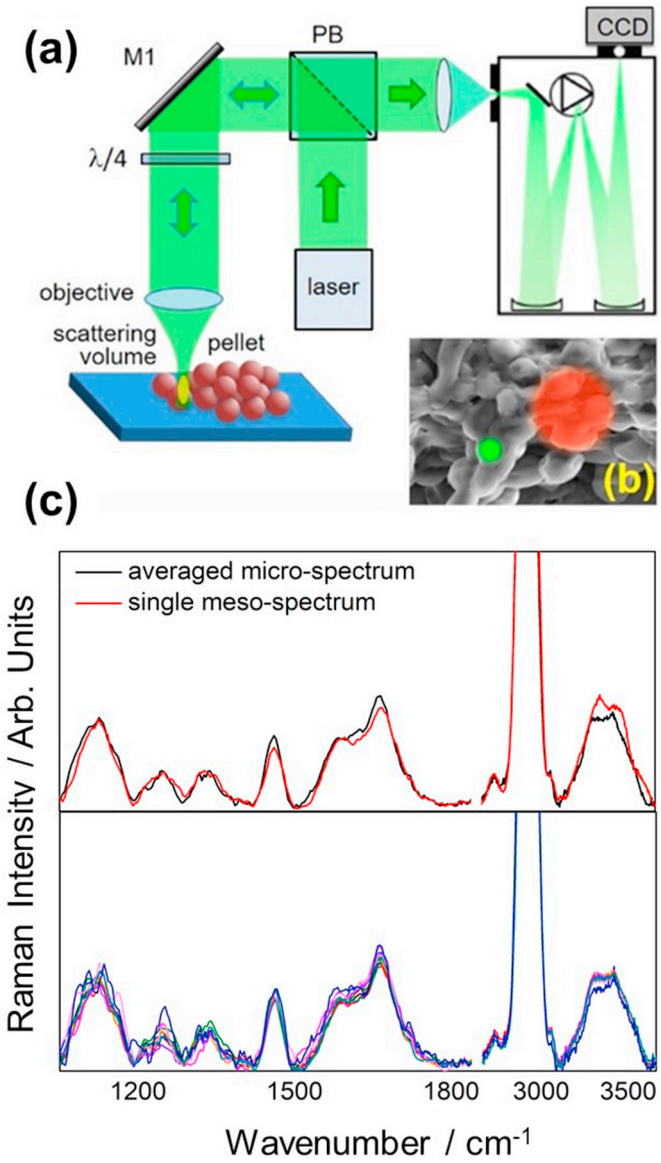

Fig. 1. a) Schematic of the Raman spectroscopy setup, part of the recently developed Brillouin-Raman micro-spectroscopy setup [39–43]. The 532 nm single mode laser beam, expanded and collimated, is reflected by a polarizing beam splitter (PB) and sent onto the sample through a lens or through a microscope objective, which is also used to collect the backscattered light. Depolarized (VH) scattered light passing through PB is analyzed by the Raman spectrometer. Alternatively, a broadband λ/4 retarder wave plate can be inserted upstream of the objective to switch from depolarized to unpolarized (VU) scattering configuration. (b) SEM micrograph of the *C.albicans* film. The green (red) dot represents the ~2 μm (~8 μm) spot of the 20× (30 mm) lens. (c) Lower panel, ten spectra obtained from random points on a yeast cells film using the 20× objective lens. Higher panel, comparison between the arithmetic average of the ten spectra (black) and a single spectrum collected by the 30 mm lens (red) on the same sample. (For interpretation of the references to colour in this figure legend, the reader is referred to the web version of this article.)

occurs for very thick pellets, also in this case possibly related to reduced heat dispersion. Good quality films were obtained by drying 20 μl drops of OD_{600} = 30 solutions, giving rise to 4–5 layered thick films of yeast cells deposited on top of polished stainless steel substrates. In these samples, fluorescence spontaneously decays in < 15 min. The residual background was estimated by a spline function and subtracted from the spectrum.

2.2. Raman measurements

Fig. 1 shows a schematic of the Raman setup. The 532 nm single mode laser beam is focused into the sample, reducing the beam intensity to < 7 mW to prevent the samples photon damage. The scattered light is collected and analyzed by a HORIBA Jobin Yvon iHR320 Triax Imaging Spectrometer, using the 600 lines/mm grating with a frequency resolution of about 10 cm^{-1}. Spectra are acquired both in unpolarized (VU) and depolarized (VH) configurations. Moreover, in order to modify the dimension of the scattering volume, two different focusing optics are used passing from microscopic to mesoscopic length scale sampling. In particular, using a 20× Mitutoyo M-Plan Apo microscopic objective, NA = 0.42, the laser spot diameter on the sample is ~2 μm, comparable with the dimension of a single yeast cell. At this length-scale, the sample is quite heterogeneous, as shown in recent Raman-Brillouin investigations of *Candida* biofilms [39–41]. The biochemical heterogeneity in molecular composition of the sample at micrometer level is highlighted by the differences in the ten Raman spectra reported in Fig. 1c, acquired from different positions at random on the same *C. tropicalis* sample. The range of variation of these spectra is comparable with the difference between spectra obtained from different species, seriously hindering the identification of the *Candida* species by means of a single micro-Raman spectrum. The solution to this problem can be found in acquiring many spectra from different points, with the aim to obtain an average spectrum representative of the average molecular structure and composition of the sample.

The main limits of this approach are the arbitrariness in the choice of the sampled points and the long time it takes to get a statistically significant sampling.

To considerably reduce the measurement time and to improve the reliability of statistical sampling, we opted for a mesoscopic optical sampling, obtained by means of a 30 mm achromatic lens, NA = 0.13, mounted in place of the microscope objective. In this case, we have a laser spot diameter of ~8 μm, a single spectrum already providing the average over about 20 cells in the irradiated film. Comparison between the arithmetic average of ten spectra obtained by the 20× microscopic objective and a single spectrum obtained using the 30 mm lens is reported in Fig. 1c.

We stress that one of the most important aims of the present work, i.e. mitigation of the sources of variation in Raman spectra, is reached by the proposed mesoscopic approach. In fact, sampling the spectra over about twenty cells, which were randomly mixed during both liquid culture and film formation, provides a good average of the different physiological states and growth phases of yeast cells by means of a single Raman measurement.

In addition, we have tested the effect of light polarization on the identification of species. Depolarized (VH) spectra have been recorded, analyzing the scattered light passing through the polarizing beam splitter (PB in Fig. 1a). Unpolarized (VU) spectra have been recorded by inserting a broadband λ/4 retarder wave plate upstream of the objective. Raman spectra obtained from *Candida* films in both VH and VU configurations are reported in Fig. 2. Notice that, due to the different symmetry of the vibrational modes of the biomolecules also caused by different chemical interaction with the local environment, the relative intensity of some Raman peaks, such as the amide I region between 1515 and 1750 cm^{-1}, and the carbohydrates region between 1020 and 1195 cm^{-1}, are different in the two configurations, especially for *C. albicans* and *C. glabrata* species. The possibility of employing depolarized Raman scattering has been already reported, both to determine molecular orientations in biochemical assemblies [44,45] and to improve biological contrast in complex biological samples, such as collagen fibrils with different orientations in human bones [46–48], and in different tissues, where cell polarity and fibers orientations are used as early markers of cancerous tissues [49].

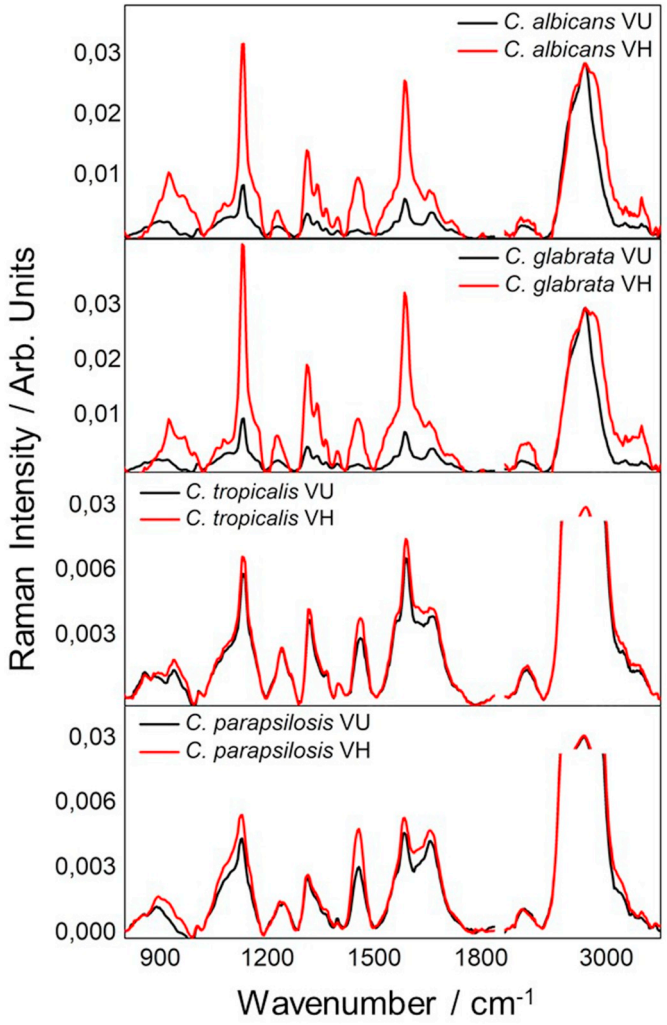

Fig. 2. Raman averaged spectra of *Candida* films, after subtraction of the fluorescent background and normalization to the intensity of the high frequency CH_2-CH_3 stretching band, recorded using the depolarized (VH, red lines) and the unpolarized (VU, black lines) configurations. (For interpretation of the references to colour in this figure legend, the reader is referred to the web version of this article.)

2.3. Multivariate analysis

Data were analyzed by principal component analysis (PCA), a multivariate statistical unsupervised method, frequently used to reduce complex multidimensional data sets to few principal components. PCA has been successfully applied to vibrational spectroscopy such as IR and Raman techniques both for mapping purposes on single cells and tissues and for microbial identification [15,23]. In fact, PCA permits not only to visualize spectra of similar variability as groups of points in a scores plot, but also to identify the key variables that generate the scores distribution. This provides precious information about the biochemical differences that cause the given distribution, although a complete biochemical characterization of the sample remains typically beyond the capabilities of PCA methods [50,51]. Commonly, PCA analysis can be applied by using the entire spectrum, with or without a baseline subtraction. In this work, we analyze the whole frequency range between 375 and 3100 cm^{-1}, excluding the "silent region" between 1780 and 2640, cm^{-1}, after the baseline subtraction and the normalization on the high frequency CH_2-CH_3 stretching band at 2800–3050 cm^{-1}. The baseline has been calculated as a spline function. This method allows to take into account not only intensity variation of well-defined peaks, but also changes in the shape of complex (convoluted) band structures.

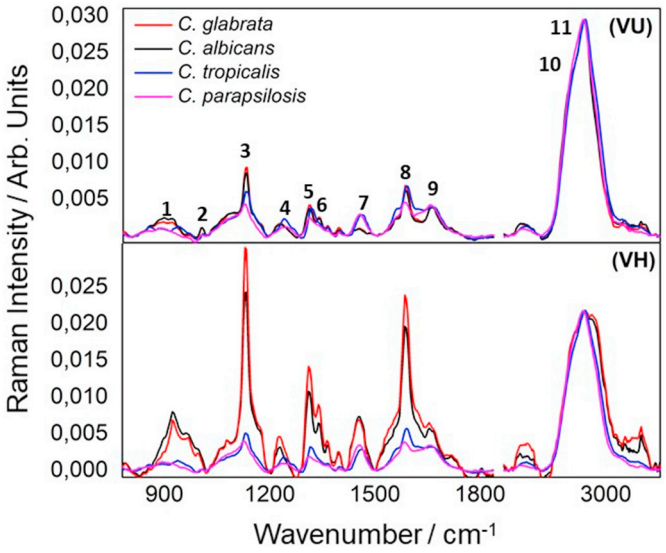

Fig. 3. Comparison of the averaged Raman spectra recorded in depolarized (upper panel) and in unpolarized (lower panel). Raman peaks can be attributed to: (1) 910 cm^{-1} glucose; (2) 1003 cm^{-1} symmetric-ring breathing of phenylalanine; (3) 1125–1128 cm^{-1} CN stretch of proteins, carbohydrates (glycogen) and cytochrome *c*; (4) 1245–1265 cm^{-1} amide III; (5) 1314 cm^{-1} cytochrome *c*; (6) 1340–1350 cm^{-1} carbohydrates and proteins; (7) 1440–1460 cm^{-1}, CH_2 deformation mode; (8) 1585 cm^{-1} guanine and adenine, cytochrome *c*; (9) 1655–1670 cm^{-1} amide I; (10) 2880 cm^{-1} CH_2 stretching lipids; (11) 2935 cm^{-1} CH_3 stretching of proteins [40].

"prcomp" and "Factoextra" open source *R* routines have been used for the PCA analysis.

3. Results and discussion

Fifty spectra were collected both in depolarized and unpolarized configurations from different volumes of each species, using a 600 lines/mm grating, 100 μm slit and a time of integration of 420 s. The mean spectrum for each species is reported in Fig. 3, showing the good signal to noise ratio in the whole investigated region 800–3100 cm^{-1}.

Already from the average spectra, it can be noticed that well defined differences are present comparing the spectra of *C. parapsilosis* and *C. tropicalis*, while the differences between *C. albicans* and *C. glabrata* are less pronounced. This observation is confirmed by the PCA analysis. The results obtained from the VU spectra are shown in Fig. 4a: the two principal components, which together account for the 80% of the data variability, are able to clearly discriminate only three different groups. In particular, PC1 distinguish *C. tropicalis* and *C. parapsilosis* (on the right side) from *C. glabrata* and *C. albicans* (on the left side). Concerning PC2, even if it is very effective in dividing *C. parapsilosis* from *C. tropicalis,* it is not able to distinguish *C. glabrata* specie from *C. albicans.*

To deepen the investigation, the PCA analysis is also performed on depolarized spectra. These spectroscopic data make it possible to improve the identification ability, as reported in the lower panel of Fig. 4b) labelled as VH. PCA score plot shows that PC1 and PC2 can now divide the samples into the four groups, even if *C. glabrata* and *C. albicans* are still quite close the one to the other. In fact, the intra-species dispersion of these two samples is quite large, and, in some cases, it is larger than the interspecies distance. We would however point out that the baseline subtraction can generally play a role in the evaluation of tiny spectral differences. In our case, if three different groups (*C. parapsilosis*, *C. tropicalis* and *C. albicans* - *C. glabrata*) are always recognized by the PCA analysis, the differentiation of *C. albicans* from *C. glabrata* can be modified by the baseline choice. To test the robustness of the obtained result we performed the PCA analysis also on the spectra prior the baseline subtraction. Also in this case, the PCA proves

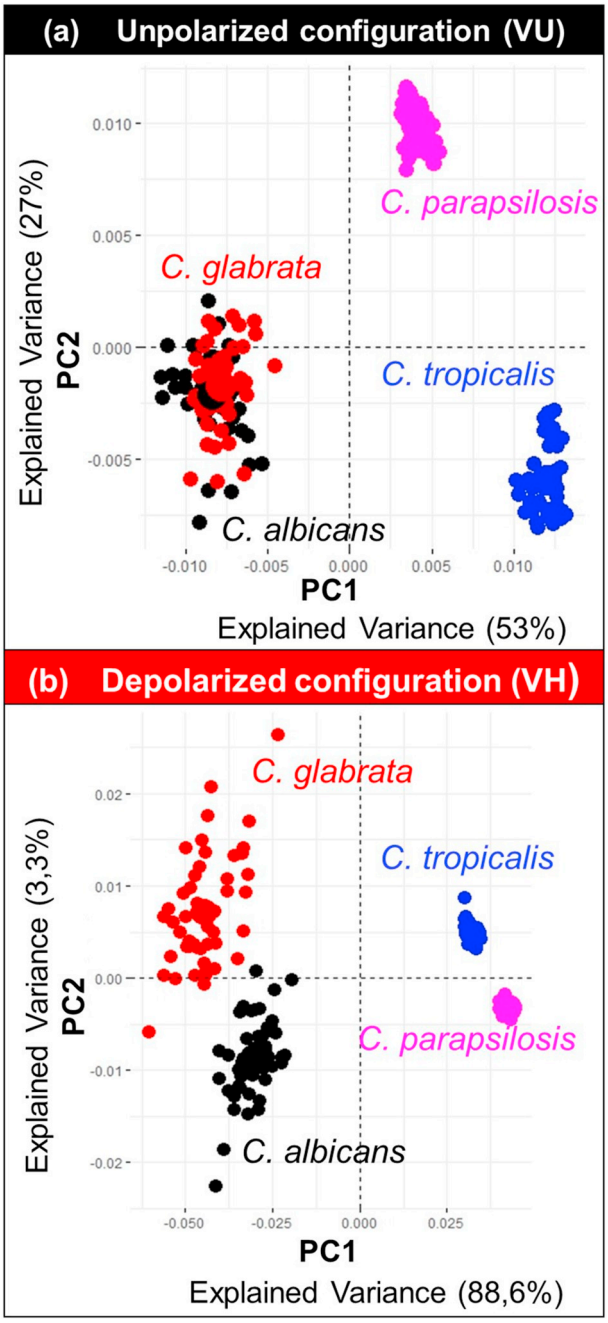

Fig. 4. PCA scores plot obtained from the VU spectra (a) and from the VH spectra (b) of the four different pellets: *C. tropicalis* (blue), *C. parapsilosis* (magenta), *C. albicans* (black) and *C. glabrata* (red). (For interpretation of the references to colour in this figure legend, the reader is referred to the web version of this article.)

able to separate the different species in the depolarized spectra.

To comment our results, it's worth to notice that: i) to reinforce the PCA analysis, spectroscopic data in different polarization can help in the species identification; ii) the dispersion of the points relative to the same species for both VU and VH configuration, is not negligible. It represents the intra-species variability, which is still detectable in spite of the collection of spectra averaged over tens cells and the optimization of the sample preparation to have a homogeneous pellet. This result probably depends on the natural heterogeneity of the eukaryotic cells. Furthermore, iii) in case of highly luminescent samples, like Candida ones, the baseline subtraction is an important procedure that has to be carefully optimized because it can modify or hide the

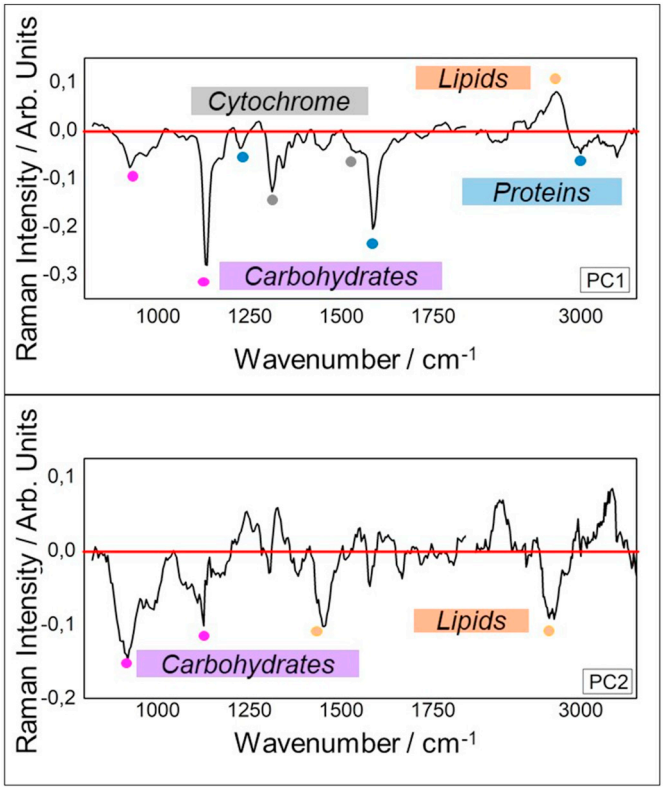

Fig. 5. Projection of the loadings plot on the PC1 (upper panel) and PC2 (lower panel) axis of the PCA plot in Fig. 4b.

differentiation of spectra.

Further useful information can be obtained by the analysis of the shape of PC1 and PC2 components, reported in Fig. 5 and obtained for the VH spectra. The first principal component, which describes about 88.6% of data variance, can distinguish *C. tropicalis* and *C. parapsilosis* from *C. albicans* and *C. glabrata* mostly because of a different relative content in proteins and lipids.

In fact, Fig. 5a shows that, besides the typical peaks attributed to proteins, such as amide I (1655–1670 cm^{-1}) and amide III (1245–1265 cm^{-1}), also the intensity of the low frequency side of the CH stretching profile with respect to the higher one (2850 vs 2935 cm^{-1}) is clearly much more represented in *C. albicans* and *C. glabrata* spectra. *The opposite behaviour* is distinctive for *C. parapsilosis* and *C. tropicalis* ones. In different biophysical frameworks it has been already highlighted how key information can be obtained by the analysis of the high frequency CH stretching band profile: the dynamical supramolecular changes in living T-lymphocytes [52], the biochemical composition in Candida biofilms [39], the aggregation process of micellar solutions [53] the sol-gel transition in lipid membranes [54] or to establish the homogeneous composition in human cornea [55]. Here the PCA analysis points out on the importance of the shape of this high frequency band also for the species identification.

The second principal component detects other features that are important to distinguish *C. glabrata* and *C. tropicalis* from *C. albicans* and *C. parapsilosis*. Fig. 5b shows that typical frequencies assignable to carbohydrates, such as 910 cm^{-1} (glucose) and 1125–1128 cm^{-1} (glycogen) as well as frequencies characteristic of the lipid component are present mostly on *C. albicans* and *C. tropicalis* spectra.

4. Conclusion

In the present work, we have explored the critical aspects in sample preparation, spectra measurements and data processing, to mitigate the sources of variation and propose a procedure for Raman phenotypical

identification of yeast cells. Best results have been obtained by means of a meso-Raman approach, in place of more traditional micro-Raman methods. Collecting scattered light by low numerical aperture optics, the meso-Raman approach directly records averages over tens of cells reducing not only the acquisition time of 10–20 times but also facilitating the data processing. The proposed procedure considerably reduces the spectral variability induced by different internal cellular portions, different metabolic states, and colony's architecture, encountered by traditional confocal Raman measurements. The use of thin pellets, made by 4–5 layers of planktonic cells deposited on top of polished stainless-steel substrates, give an almost homogeneous sample, with a tolerable fluorescence background. In this condition, a PCA analysis of the intensity of depolarized Raman spectra is able to differentiate the most common *Candida* species, namely *C. glabrata*, *C. albicans*, *C. parapsilosis* and *C. tropicalis*. These four species form two genetically distant clusters, being *C. glabrata* a post WGD whereas the other three are pre WGD species. The proposed method can be successfully used to separate strains of different species, but it is not likely to serve as a phylogenetic tool.

In fact, it is interesting to notice that Raman identification is quite easy for *C. parapsilosis* and *C. tropicalis*, while the spectroscopic signatures of *C. glabrata* and *C. albicans* are quite similar even if they are phylogenetically and genetically very different. The use of VH spectra and the correct background subtraction helped in their identification.

Moreover, the dispersion of points relative to the same species in the PCA plot suggests that Raman spectra are still sensitive to the metabolic state of yeast cells, even after the average performed by the chosen optical configuration, which integrate over tens of cells. On one hand, these results stimulate the research of algorithms and statistical treatments to improve the taxonomic resolution also when several strains of the same species are considered. On the other hand, these results could indicate the future use of the technique to cluster strains not only within taxonomic categories, but also within functional groupings, such as the strains able to form biofilm [26,56], or to resist to drugs [57].

It is worth noting that the setup required for mesoscopic Raman measurements is quite inexpensive since it does not even need a microscopy stage and, at the same time, low biomass amounts, obtainable in few hours of incubation, can be used for the proposed meso-Raman approach. Finally, this approach does not require the careful - guided by eye - selection of the portion of cell to be irradiated, typical of a micro-Raman approach, suggesting the possibility for the large-scale use of Raman spectroscopy for microbial identification.

Acknowledgements

The authors acknowledge the support from Gilead Fellowship Project “Caratterizzazione del biofilm ed efficacia del trattamento con Amfotericina B liposomiale in ceppi filmogeni del gruppo Candida parapsilosis sensu lato” (URL: http://www.itfellowshipprogram.it).

References

[1] D. Naumann, D. Helm, H. Labischinski, Microbiological characterizations by FT-IR spectroscopy, Nature 351 (6321) (1991) 81–82.
[2] L.-P. Choo-Smith, K. Maquelin, T. Van Vreeswijk, et al., Investigating microbial (micro) colony heterogeneity by vibrational spectroscopy, Appl. Environ. Microbiol. 67 (4) (2001) 1461–1469.
[3] C. Kirschner, K. Maquelin, P. Pina, et al., Classification and identification of enterococci: a comparative phenotypic, genotypic, and vibrational spectroscopic study, J. Clin. Microbiol. 39 (5) (2001) 1763–1770.
[4] C. Sandt, G. Sockalingum, D. Aubert, et al., Use of Fourier-transform infrared spectroscopy for typing of Candida albicans strains isolated in intensive care units, J. Clin. Microbiol. 41 (3) (2003) 954–959.
[5] M. Harz, P. Rösch, J. Popp, Vibrational spectroscopy—a powerful tool for the rapid identification of microbial cells at the single-cell level, Cytometry A. 75 (2) (2009) 104–113.
[6] M. Kümmerle, S. Scherer, H. Seiler, Rapid and reliable identification of food-borne yeasts by Fourier-transform infrared spectroscopy, Appl. Environ. Microbiol. 64 (6) (1998) 2207–2214.
[7] I. Notingher, L.L. Hench, Raman microspectroscopy: a noninvasive tool for studies of individual living cells in vitro, Expert Rev. Med. Devices. 3 (2) (2006) 215–234.
[8] C.L. Schoch, K.A. Seifert, S. Huhndorf, et al., Nuclear ribosomal internal transcribed spacer (ITS) region as a universal DNA barcode marker for Fungi, Proc. Natl. Acad. Sci. 109 (16) (2012) 6241–6246.
[9] C. Colabella, L. Corte, L. Roscini, et al., Merging FT-IR and NGS for simultaneous phenotypic and genotypic identification of pathogenic Candida species, PLoS ONE 12 (12) (2017) e0188104.
[10] S. Stöckel, J. Kirchhoff, U. Neugebauer, P. Rösch, J. Popp, The application of Raman spectroscopy for the detection and identification of microorganisms, J. Raman Spectrosc. 47 (1) (2016) 89–109.
[11] K. Maquelin, C. Kirschner, L.-P. Choo-Smith, et al., Identification of medically relevant microorganisms by vibrational spectroscopy, J. Microbiol. Methods 51 (3) (2002) 255–271.
[12] S. Caponi, S. Mattana, M. Ricci, et al., Raman micro-spectroscopy study of living SH-SY5Y cells adhering on different substrates, Biophys. Chem. 208 (2016) 48–53.
[13] L. Corte, L. Roscini, C. Colabella, et al., Exploring ecological modelling to investigate factors governing the colonization success in nosocomial environment of Candida albicans and other pathogenic yeasts, Sci. Rep. 6 (2016) 26860.
[14] L. Roscini, L. Corte, L. Antonielli, P. Rellini, F. Fatichenti, G. Cardinali, Influence of cell geometry and number of replicas in the reproducibility of whole cell FTIR analysis, Analyst 135 (8) (2010) 2099–2105.
[15] K. Mlynáriková, O. Samek, S. Bernatová, et al., Influence of culture media on microbial fingerprints using Raman spectroscopy, Sensors 15 (11) (2015) 29635–29647.
[16] M. Harz, P. Rösch, K.-D. Peschke, O. Ronneberger, H. Burkhardt, J. Popp, Micro-Raman spectroscopic identification of bacterial cells of the genus Staphylococcus and dependence on their cultivation conditions, Analyst 130 (11) (2005) 1543–1550.
[17] D.S. Read, A.S. Whiteley, Chemical fixation methods for Raman spectroscopy-based analysis of bacteria, J. Microbiol. Methods 109 (2015) 79–83.
[18] M.F. Escoriza, J.M. Van Briesen, S. Stewart, J. Maier, Raman spectroscopic discrimination of cell response to chemical and physical inactivation, Appl. Spectrosc. 61 (8) (2007) 812–823.
[19] M. Ibelings, K. Maquelin, H.P. Endtz, H. Bruining, G. Puppels, Rapid identification of Candida spp. in peritonitis patients by Raman spectroscopy, Clin. Microbiol. Infect. 11 (5) (2005) 353–358.
[20] K. Maquelin, C. Kirschner, L.-P. Choo-Smith, et al., Prospective study of the performance of vibrational spectroscopies for rapid identification of bacterial and fungal pathogens recovered from blood cultures, J. Clin. Microbiol. 41 (1) (2003) 324–329.
[21] P. Rösch, M. Harz, K.D. Peschke, O. Ronneberger, H. Burkhardt, J. Popp, Identification of single eukaryotic cells with micro-Raman spectroscopy, Biopolymers 82 (4) (2006) 312–316.
[22] K. Maquelin, L.-P. Choo-Smith, H.P. Endtz, H. Bruining, G. Puppels, Rapid identification of Candida species by confocal Raman microspectroscopy, J. Clin. Microbiol. 40 (2) (2002) 594–600.
[23] N.S. Chouthai, A.A. Shah, H. Salimnia, et al., Use of Raman spectroscopy to decrease time for identifying the species of Candida growth in cultures, Avicenna J. Med. Biotechnol. 7 (1) (2015) 45.
[24] I. Espagnon, D. Ostrovskii, R. Mathey, et al., Direct identification of clinically relevant bacterial and yeast microcolonies and macrocolonies on solid culture media by Raman spectroscopy, J. Biomed. Opt. 19 (2) (2014) 027004.
[25] K. Rebrošová, M. Šiler, O. Samek, et al., Rapid identification of staphylococci by Raman spectroscopy, Sci. Rep. 7 (1) (2017) 14846.
[26] O. Samek, K. Mlynariková, S. Bernatová, et al., Candida parapsilosis biofilm identification by Raman spectroscopy, Int. J. Mol. Sci. 15 (12) (2014) 23924–23935.
[27] P. Rösch, M. Harz, M. Schmitt, J. Popp, Raman spectroscopic identification of single yeast cells, J. Raman Spectrosc. 36 (5) (2005) 377–379.
[28] S. Kloß, B. Kampe, S. Sachse, et al., Culture independent Raman spectroscopic identification of urinary tract infection pathogens: a proof of principle study, Anal. Chem. 85 (20) (2013) 9610–9616.
[29] C. Sandt, T. Smith-Palmer, J. Pink, L. Brennan, D. Pink, Confocal Raman microspectroscopy as a tool for studying the chemical heterogeneities of biofilms in situ, J. Appl. Microbiol. 103 (5) (2007) 1808–1820.
[30] B. Dujon, D. Sherman, G. Fischer, et al., Genome evolution in yeasts, Nature 430 (6995) (2004) 35.
[31] P. Eggimann, J. Garbino, D. Pittet, Epidemiology of Candida species infections in critically ill non-immunosuppressed patients, Lancet Infect. Dis. 3 (11) (2003) 685–702.
[32] M. Pfaller, D. Diekema, Epidemiology of invasive candidiasis: a persistent public health problem, Clin. Microbiol. Rev. 20 (1) (2007) 133–163.
[33] P. Montravers, J.P. Mira, J.P. Gangneux, O. Leroy, O. Lortholary, A.S. Group, A multicentre study of antifungal strategies and outcome of Candida spp. peritonitis in intensive-care units, Clin. Microbiol. Infect. 17 (7) (2011) 1061–1067.
[34] G. Ramage, S.P. Saville, D.P. Thomas, J.L. Lopez-Ribot, Candida biofilms: an update, Eukaryot. Cell 4 (4) (2005) 633–638.
[35] C. Seneviratne, L. Jin, L. Samaranayake, Biofilm lifestyle of Candida: a mini review, Oral Dis. 14 (7) (2008) 582–590.
[36] J. Chandra, D.M. Kuhn, P.K. Mukherjee, L.L. Hoyer, T. Mccormick, M.A. Ghannoum, Biofilm formation by the fungal pathogenCandida albicans: development, architecture, and drug resistance, J. Bacteriol. 183 (18) (2001) 5385–5394.
[37] J. Sardi, L. Scorzoni, T. Bernardi, A. Fusco-Almeida, M.M. Giannini, Candida species: current epidemiology, pathogenicity, biofilm formation, natural antifungal products and new therapeutic options, J. Med. Microbiol. 62 (1) (2013) 10–24.
[38] A.K. Kniggendorf, T.W. Gaul, M. Meinhardt-Wollweber, Effects of ethanol,

formaldehyde, and gentle heat fixation in confocal resonance Raman microscopy of purple nonsulfur bacteria, Microsc. Res. Tech. 74 (2) (2011) 177–183.
[39] L. Roscini, A. Vassiliou, L. Corte, et al., Yeast biofilm as a bridge between medical and environmental microbiology across different detection techniques, Infect. Dis. Ther. 7 (1) (2018) 27–34.
[40] S. Mattana, M.A. Cardinali, S. Caponi, et al., High-contrast Brillouin and Raman micro-spectroscopy for simultaneous mechanical and chemical investigation of microbial biofilms, Biophys. Chem. 229 (2017) 123–129.
[41] F. Scarponi, S. Mattana, S. Corezzi, et al., High-performance versatile setup for simultaneous Brillouin-Raman microspectroscopy, Phys. Rev. X 7 (3) (2017) 031015.
[42] S. Mattana, S. Caponi, F. Tamagnini, D. Fioretto, F. Palombo, Viscoelasticity of amyloid plaques in transgenic mouse brain studied by Brillouin microspectroscopy and correlative Raman analysis, J. Innov. Opt. Health Sci. 10 (06) (2017) 1742001.
[43] S. Mattana, M. Mattarelli, L. Urbanelli, et al., Non-contact mechanical and chemical analysis of single living cells by microspectroscopic techniques, Light: Sci. Appl. 7 (2) (2018) 17139.
[44] M. Tsuboi, J.M. Benevides, G.J. Thomas Jr., Raman tensors and their application in structural studies of biological systems, Proceed. Jpn. Acad. Ser. B 85 (3) (2009) 83–97.
[45] M. Tsuboi, J.M. Benevides, P. Bondre, G.J. Thomas, Structural details of the thermophilic filamentous bacteriophage PH75 determined by polarized Raman microspectroscopy, Biochemistry 44 (12) (2005) 4861–4869.
[46] M. Kazanci, P. Roschger, E. Paschalis, K. Klaushofer, P. Fratzl, Bone osteonal tissues by Raman spectral mapping: orientation–composition, J. Struct. Biol. 156 (3) (2006) 489–496.
[47] S. Schrof, P. Varga, L. Galvis, K. Raum, A. Masic, 3D Raman mapping of the collagen fibril orientation in human osteonal lamellae, J. Struct. Biol. 187 (3) (2014) 266–275.
[48] B. Gong, M.D. Morris, Raman spectroscopy monitors adverse bone sequelae of cancer radiotherapy, Chin. Chem. Lett. 26 (4) (2015) 401–406.
[49] H. Abramczyk, B. Brozek-Pluska, M. Kopec, Polarized Raman microscopy imaging: capabilities and challenges for cancer research, J. Mol. Liq. 259 (2018) 102–111.
[50] F. Bonnier, H. Byrne, Understanding the molecular information contained in principal component analysis of vibrational spectra of biological systems, Analyst 137 (2) (2012) 322–332.
[51] H. Shinzawa, K. Awa, W. Kanematsu, Y. Ozaki, Multivariate data analysis for Raman spectroscopic imaging, Journal of Raman Spectroscopy: An International Journal for Original Work in all Aspects of Raman Spectroscopy, Including Higher Order Processes, and also Brillouin and Rayleigh Scattering 40 (12) (2009) 1720–1725.
[52] S. Caponi, L. Liguori, A. Giugliarelli, et al., Raman micro-spectroscopy: a powerful tool for the monitoring of dynamic supramolecular changes in living cells, Biophys. Chem. 182 (2013) 58–63.
[53] S. Caponi, S. Mattana, M. Ricci, et al., A multidisciplinary approach to study the functional properties of neuron-like cell models constituting a living bio-hybrid system: SH-SY5Y cells adhering to PANI substrate, AIP Adv. 6 (11) (2016) 111303.
[54] P. Sassi, S. Caponi, M. Ricci, et al., Infrared versus light scattering techniques to monitor the gel to liquid crystal phase transition in lipid membranes, J. Raman Spectrosc. 46 (7) (2015) 644–651.
[55] R. Mercatelli, S. Mattana, L. Capozzoli, et al., Morpho-mechanics of human collagen superstructures revealed by all-optical correlative micro-spectroscopies, Comm. Biol. 2 (2019) 117.
[56] W.E. Huang, S. Ude, A.J. Spiers, Pseudomonas fluorescens SBW25 biofilm and planktonic cells have differentiable Raman spectral profiles, Microb. Ecol. 53 (3) (2007) 471–474.
[57] T.Y. Liu, K.T. Tsai, H.H. Wang, Functionalized arrays of Raman-enhancing nanoparticles for capture and culture-free analysis of bacteria in human blood, Nat. Commun. 2 (2011) 538.